



# Multiple morphologies of ZnO films synthesized on flexible poly(ethylene terephthalate) by electroless deposition

Zhenggao Fu<sup>a</sup>, Zhanchang Pan<sup>a</sup>, Dalei Sun<sup>a,\*</sup>, Guohe Zhan<sup>a</sup>, Huangchu Zhang<sup>b</sup>, Xiangfu Zeng<sup>b</sup>, Guanghui Hu<sup>a</sup>, Chumin Xiao<sup>a</sup>, Zhigang Wei<sup>a</sup>

<sup>a</sup> School of Chemical Engineering and Light Industry, Guangdong University of Technology, Guangzhou, Guangdong 510006, China

<sup>b</sup> Victory Giant Technology (Hui Zhou) Co., Ltd, Huizhou 516083, China

## ARTICLE INFO

### Article history:

Received 15 April 2016

Received in revised form

9 June 2016

Accepted 10 August 2016

Available online 11 August 2016

### Keywords:

ZnO films

Multiple morphologies

Electroless deposition

Optical property

Sheet resistance

## ABSTRACT

Multiple morphologies of ZnO films were synthesized on flexible poly(ethylene terephthalate) (PET) by electroless deposition, using  $\text{Zn}(\text{NO}_3)_2$  and dimethylamineborane(DMAB) solutions. ZnO nanorods, nanohexagonal prisms and microflakes films can be obtained by adjusting  $\text{Zn}(\text{NO}_3)_2$  concentration. The XRD results revealed the ZnO films have a wurtzite structure. The room-temperature photoluminescence (PL) spectra of ZnO/PET films exhibited dominated purple peak, negligible blue and green peak, indicating an excellent optical property. Sheet resistance of ZnO/PET films decreased from  $1.04 \times 10^6$  to  $6.42 \times 10^5 \Omega/\text{sq.}$  as the grain size of the ZnO crystals grew up. Furthermore, hydrogen separation theory was put forward in the deposition process. The knowledge acquired in this work is significant for the ZnO films with applications in optoelectronic devices.

© 2016 Elsevier B.V. All rights reserved.

## 1. Introduction

Metal oxides are multifunctional materials with a variety of applications. Specially, zinc oxide (ZnO) can be considered as the most important one among all various metal oxides due to the wide band gap (3.36 eV) and large exciton binding energy (60 meV) [1]. These characteristics make this material interesting for many applications such as dye-sensitized solar cells [2], piezoelectric materials [3], energy storage devices [4], and photocatalyst materials [5]. To obtain high quality ZnO materials, various methods have been reported in the literatures, such as magnetron sputtering [6], pulsed laser deposition [7], chemical vapor deposition [8], sol-gel growth method [5], and hydrothermal method [9]. Recently, the electroless deposition (ELD) method has attracted more and more attention for its significant advantages, such as low operation temperature (below 90 °C), scalable process, simple manipulation, easy control and uniform products [10].

Herein, we fabricated ZnO films on PET substrate at 70 °C by a new ELD method. This approach with simple and effective pretreatment of the substrate is relatively efficient in comparison with the traditional ELD route [10]. The new process mainly involves five steps: degreasing, roughening, sensitization, activation and

deposition. The deposition of ZnO films takes place in  $\text{Zn}(\text{NO}_3)_2$ -DMAB solutions, and ZnO nanorods, nanohexagonal prisms, and microflakes films can be obtained with increasing the concentration of  $\text{Zn}(\text{NO}_3)_2$ . The desired optical and electrical properties were achieved due to the uniform thickness and size distribution of the samples. ZnO/PET films is very helpful for designing various optoelectronic devices, since PET is a typical flexible substrate and exhibits enormous applications [11].

## 2. Experimental details

### 2.1. Preparation of ZnO/PET films

PET films (DuPont Mylar, 50 μm) were used as substrate and degreased by immersing in an alkaline degreasing solvent at 50 °C for 15 min, and cleaned ultrasonically in deionized water for 10 min.

The degreased films were immersed in 200 g/L NaOH solution at 80 °C for 50 min, while 50 mL/min  $\text{O}_3$  was introduced continuously. The surface of PET films achieved good wettability after roughening, which made it rough enough to adsorb the catalyst and enhance the adhesion.

Surface sensitization and activation were successively conducted by immersing the roughened films in a solution containing

\* Corresponding author.

E-mail addresses: [fuzg1990@126.com](mailto:fuzg1990@126.com) (Z. Fu), [sdlei80@163.com](mailto:sdlei80@163.com) (D. Sun).

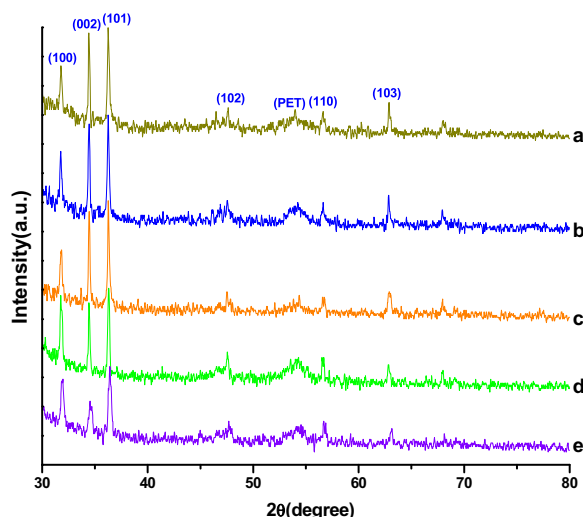


Fig. 1. XRD patterns of ZnO samples with different  $\text{Zn}(\text{NO}_3)_2$  concentrations. (a: 0.005 M, b: 0.008 M, c: 0.01 M, d: 0.05 M, e: 0.10 M).

**Table 1**  
Structural parameters obtained from the XRD patterns shown in Fig. 1.

Sample name	(hkl)	$2\theta$ (°)	FWHM (°)	Crystallite size (nm)
0.005 M	101	36.260	0.264	34.3
0.008 M	101	36.260	0.209	45.6
0.01 M	101	36.263	0.218	43.1
0.05 M	101	36.319	0.234	39.6
0.10 M	101	36.438	0.358	24.3

$\text{SnCl}_2$  (20 g/L),  $\text{HCl}$  (60 mL/L 37%) and  $\text{PdCl}_2$  (0.1 g/L),  $\text{HCl}$  (20 mL/L 37%) at room temperature for 5 min.

The catalyzed films were immersed into a 100 mL beaker containing 0.005–0.1 M  $\text{Zn}(\text{NO}_3)_2$  and 0.01 M DMAB solutions at 70 °C for 2 h to deposit ZnO crystals. Finally, the films obtained were rinsed with deionized water and dried in 60 °C oven.

## 2.2. Characterization of ZnO/PET films

The surface morphology of ZnO/PET films were observed by scanning electron microscope (SEM), and the crystalline structure characterization were evaluated by X-ray diffraction ( $\lambda=0.15405$  nm, Rigaku-Ultima III). The optical properties were measured by the photoluminescence (PL, He-Cd laser, 325 nm). The four-point probe technique (ST-2258C, China) was used to determine the sheet resistance.

## 3. Results and discussions

Fig. 1 shows the XRD patterns of ZnO samples with different  $\text{Zn}(\text{NO}_3)_2$  concentrations. The positions of the diffraction peaks indicate that all the crystals were polycrystalline with a structure that belonged to the wurtzite structure ZnO (JCPDS data card 36-1451). The crystallite size for the (101) plane diffraction peak of ZnO crystals has been calculated by using the Scherrer formula

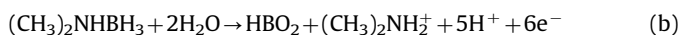
[12] and the results are shown in Table 1. As a whole, with increasing  $\text{Zn}(\text{NO}_3)_2$  concentration, the diffraction angles are recognized slightly shifted to high-angle and the crystallite size gradually decreases, suggesting that the ZnO films include somewhat surface defects [13].

To explore the change of ZnO morphologies, various precursor concentrations were investigated. Fig. 2a–e shows a series of ZnO grown at different concentrations, such as 0.005 M, 0.008 M, 0.01 M, 0.05 M and 0.10 M. It is observed that the morphology of the ZnO depends on  $\text{Zn}(\text{NO}_3)_2$  concentration. It can be clearly seen that the morphologies of the synthesized samples changed from nanorods to nanohexagonal prisms, then to microflakes. Besides, the grain size of the ZnO crystals grows increasingly with the increase of  $\text{Zn}(\text{NO}_3)_2$  concentration. Under low  $\text{Zn}(\text{NO}_3)_2$  concentrations, dense ZnO crystals show clear 1D nanostructures (Fig. 2a–c), and the nanohexagonal prisms grow and gather to form microflakes when the concentration ranging from 0.01 to 0.05 M (Fig. 2d). Finally, ZnO structure films are completely turned to 2D microflakes when the concentration increased to 0.10 M (Fig. 2e).

The room-temperature PL spectra of ZnO samples are shown in Fig. 3a. A strong purple band peak at ca. 390 nm along with weak blue and green band peaks centered at ca. 465 nm and ca. 540 nm are observed, respectively. It is generally agreed that excitonic recombination corresponding to the near-band-edge (NBE) emission of ZnO leads to the appearance of purple emission while the weak blue and green emission peaks are commonly referred to the defects such as oxygen vacancies and interstitial Zn [14]. And the high ratio of the UV PL intensity implies good optical properties. As  $\text{Zn}(\text{NO}_3)_2$  concentration increased, PL peaks exhibited a blue-shift which may be ascribed to size effect and their unique morphologies [12].

Fig. 3b shows sheet resistance of ZnO films with different  $\text{Zn}(\text{NO}_3)_2$  concentrations. The vertical red lines are error bars. The deposited ZnO films had sheet resistance of  $1.04 \times 10^6$ ,  $9.97 \times 10^5$ ,  $9.02 \times 10^5$ ,  $7.99 \times 10^5$  and  $6.42 \times 10^5 \Omega/\text{sq.}$ , respectively. The dramatic decreases in sheet resistance are mainly due to size effect. In other words, specific ZnO morphologies may contribute to decrease sheet resistance. With increasing  $\text{Zn}(\text{NO}_3)_2$  concentration, the grain size of the ZnO crystals grows larger quickly. ZnO films consisting of bigger grains have fewer grain boundaries to impede electron motion, so they show higher electrical conductivity [15].

The electroless deposition mechanism is not clear. Generally, it is believed that the deposition reactions can be described by the following schemes [11]:



However, in the experiment we found many bubbles were produced and adsorbed on the surface of PET films when the catalyzed films were immersed in electroless deposition solutions. Besides, pH value of the solutions would rise after electroless deposition. Gas chromatogram confirmed that the bubble (gas) is  $\text{H}_2$  only. These results indicated  $\text{H}^+$  in the solutions were converted

Download English Version:

<https://daneshyari.com/en/article/8016118>

Download Persian Version:

<https://daneshyari.com/article/8016118>

[Daneshyari.com](https://daneshyari.com)